

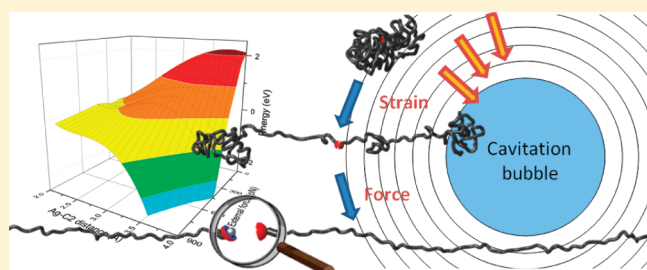
Unfolding and Mechanochemical Scission of Supramolecular Polymers Containing a Metal–Ligand Coordination Bond

Ramon Groote,^{†,‡} Bartłomiej M. Szyja,[§] Evgeny A. Pidko,^{‡,§} Emiel J. M. Hensen,[§] and Rint P. Sijbesma^{*,†,‡}[†]Laboratory of Macromolecular and Organic Chemistry, [‡]Institute for Complex Molecular Systems, and [§]Schuit Institute of Catalysis, Eindhoven University of Technology, P.O. Box 513, 5600 MB Eindhoven, The Netherlands

Supporting Information

ABSTRACT: Mechanochemical scission of supramolecular polymer complexes by ultrasound is investigated using viscosity measurements and molecular dynamics (MD) simulations combined with constrained geometry optimization (COGEF) calculations. The supramolecular polymers used in this study consist of a poly(tetrahydrofuran) (PTHF) backbone that contains a silver(I)–NHC (NHC = *N*-heterocyclic carbene) coordination complex in the chain center. The limiting molecular weight (M_{lim}) for mechanochemical chain scission is lower for supramolecular polymers than for their covalent analogues.

The longest characteristic relaxation times of the supramolecular polymers were obtained from viscosity measurements, and they confirmed that the criterion for coil-to-stretch is fulfilled in typical sonication experiments. A model DFT study was performed to estimate the value of external force that is required to break a silver(I)–NHC coordination bond. A combination of *ab initio* MD simulations and COGEF provided an atomistic insight into the response of the supramolecular center of the polymer chain to external force. The calculations indicated that the force required to break the chain is between 400 and 500 pN. This is significantly lower than the force of several nN that is typically required to break e.g. covalent C–C bonds in polymer backbones. These results confirm that the reduction in M_{lim} is due to the lower bond strength of the metal–ligand coordination bonds as compared to covalent bonds.



INTRODUCTION

We studied the physical aspects of mechanochemical scission in supramolecular polymers that incorporate a metal–ligand coordination bond at the central position within their polymer backbone. We investigated the coil-to-stretch transition of these supramolecular polymers under the influence of a (hydrodynamic) force field as well as their consecutive mechanochemical scission pathway in order to get a better understanding of the mechanisms and processes underlying their use as mechanically activated catalysts.^{1–3} In addition, these new insights will be useful and necessary for creating a framework that allows for rational design of new experiments and the exploration of alternative methods for mechanochemical activation beyond ultrasound.² It was verified both experimentally and numerically that the incorporation of a weak metal–ligand coordination bond within the polymer backbone significantly enhances mechanochemical scission efficiency. This is in full agreement with earlier work where a significant reduction in the limiting molecular weight (M_{lim}) for mechanochemical chain scission was observed for supramolecular polymers compared to their fully covalent analogues.^{1,2,4}

Polymer mechanochemistry has a long history that started in 1934 when the German scientist Hermann Staudinger first reported about mechanical degradation of polymers. He observed that the molecular weight of polymers decreased under mastication.⁶ In the decades that followed mechanical degradation

of polymers using various experimental setups was studied extensively.^{7,8} Perhaps the most elaborate and detailed set of studies was carried out in the 1980s and 1990s by the groups of Odell and Keller^{9,10} and Nguyen and Kausch.¹¹ Both groups studied the kinetics and mechanisms of mechanochemical scission of polymers in solution using different types of hydrodynamic flows created by various, tailor-made hydrodynamic flow devices. More recently, polymer mechanochemistry has gained a lot of interest for its ability to mechanically activate specific reactive groups (commonly referred to as “mechanophores”) within polymer chains. It has turned out that mechanochemical scission of polymer chains always occurs around the center of the polymer chains due to accumulation of force along the polymer backbone,^{7,9–11} provided that the molecular weight of the polymer chain is higher than a certain limiting molecular weight (M_{lim}) for mechanochemical chain scission.^{8,10,12} However, the characteristic midpoint scission can be altered by the incorporation of weak bond at off-center position within the polymer chain as shown by the work of Encina et al.¹³ and Berkowski et al.¹⁴ Thus, the preferential site for mechanochemical chain scission can be tailored by design of the structure of the polymer backbone.

Received: July 26, 2011

Revised: November 1, 2011

Published: November 16, 2011

Site-specific activation of mechanophores opens the way for a whole new class of mechanoresponsive materials that allow for carrying out chemical transformations using mechanical forces instead of more conventional methods, including thermal and (photo)chemical activation. Examples of such mechanoresponsive behavior include color changes of polymer samples upon deformation,¹⁵ stress relief through mechanically triggered intramolecular rearrangements,¹⁶ and even mechanically activated catalysis (“mechanocatalysis”).^{1–3} The latter two of these systems are of potential interest for applications in autonomous self-healing materials. The work of various research groups throughout the world has clearly demonstrated that mechanically activated chemical reactions often proceed via different reaction pathways and may result in completely different reaction products when compared to their thermally activated analogues.^{17–19}

A convenient method for imposing hydrodynamic force onto polymers in solution is by subjecting the polymer solution to ultrasound.⁷ When using ultrasound for breaking polymer chains, the hydrodynamic forces arise from a strong extensional flow field in solution upon collapse of a cavitation bubble.²⁰ The extensional forces are highest close to the interface of the collapsing cavitation bubble and become lower at a distance further away in solution. As a result of the extensional forces, the polymer chains which are present in the generated force field will undergo a coil-to-stretch transition. When the polymer chains are fully uncoiled, further stretching will result in elongation of individual chemical bonds and eventually, when the forces are high enough, mechanochemical bond scission.

Compared to their fully covalent analogues, supramolecular polymers have a much lower limiting molecular weight for mechanochemical chain scission.^{1,4,12,20} Earlier work from our group on ultrasound-induced mechanochemical scission of supramolecular polymers has demonstrated that the polymers underwent efficient mechanochemical scission at molecular weights well below M_{lim} of covalent poly(tetrahydrofuran) (PTHF) when a palladium(II)–phosphine was incorporated near the chain center.⁴ Similar observations were made in later work on silver(I)–NHC (NHC = *N*-heterocyclic carbene) supramolecular polymer complexes. For these complexes molecular weights below 10 kg mol^{-1} were already sufficient to allow mechanochemical scission to occur.^{1,2,21} Mechanochemical scission of covalent polymers is sometimes facilitated by the presence of radicals.²² However, in recent work,²¹ we demonstrated that for the supramolecular polymers studied here, the chain scission efficiency was not affected by the presence of radicals. In the current paper, we try to answer two important issues that remained unanswered. (i) Is the low observed M_{lim} compatible with a mechanism that requires uncoiling of the polymers prior to chain scission? In other words, is the relaxation time of these short polymer chains long enough for them to be uncoiled with the strain rates prevalent in ultrasonicated solutions? (ii) Is the mechanical force induced by ultrasound sufficient to break the ligand–metal bond without stabilization of the transition state by coordination with a solvent or water molecule, a process we would like to call chemically facilitated scission?

The uncoiling of the supramolecular polymers was studied by viscosity measurements in order to determine the longest characteristic relaxation times of the polymer chains. These results were then compared to the typical conditions obtained in ultrasound experiments²¹ and the uncoiling behavior of the corresponding covalent polymers in solution. The bond strengths obtained from molecular dynamics simulations in combination

with constrained geometry optimization (COGEF) calculations will indicate whether the silver(I)–NHC bond can be broken purely mechanochemical under the prevalent conditions in ultrasound experiments or if facilitation of mechanochemical bond scission by any chemically facilitated process is required.

THEORETICAL BACKGROUND

The Coil-to-Stretch Transition of Polymer Chains under Force. Before individual chemical bonds in a polymer chain can be elongated and broken, the polymer chain should first be (partially) uncoiled.¹¹ The so-called coil-to-stretch transition (abbreviated with $C \rightarrow S$) is the first crucial step that precedes mechanochemical scission of polymer chains. In hydrodynamic flows, coil-to-stretch transition from a (random) coil to a fully stretched or partially uncoiled state occurs as a result of extensional force and/or shear forces in the fluid. The process of coil-to-stretch transition is governed by the dimensionless Deborah number, De :^{23–25}

$$De = \dot{\epsilon} \lambda_0 \quad (1)$$

De (sometimes also referred to as Weissenberg number, Wi) gives the ratio between the two characteristic time scales involved in the uncoiling of a polymer chain, being the extensional rate in the solution $\dot{\epsilon}$ (being equal to the velocity gradient in the solution) and the longest characteristic relaxation mode or relaxation time λ_0 of the polymer chain. The longest characteristic relaxation mode of the polymer chain represents the relaxation of the full end-to-end vector of the polymer chain (i.e., relaxation of the polymer chain as a whole). If the polymer chain is considered as an elastic spring on which an extensional force is acting through viscous coupling with a solvent, the coil-to-stretch transition occurs when the value of De fulfills the following criterion:^{23,25}

$$De_{crit} = 1/2 \quad (2)$$

From this criterion it follows that, since λ_0 has a fixed value for a given polymer chain in a particular solvent, coil-to-stretch transition occurs when the critical extensional rate is exceeded:

$$\dot{\epsilon}_{crit} = \frac{1}{2\lambda_0} \quad (3)$$

At extensional rates below the critical value, the relaxation of the polymer chain is faster than the speed of extension. This means that at lower rates of extension the polymer chain cannot be fully extended before it relaxes back to its (random) coil conformation. Hysteresis is present between coil-to-stretch ($C \rightarrow S$) and stretch-to-coil ($S \rightarrow C$) transition of a polymer chain in solution under the influence of extensional forces. This is caused by a difference in the longest relaxation time for a polymer chain in its unperturbed coiled state (which is the characteristic relaxation time for the $C \rightarrow S$ transition) and that of a fully extended polymer chain (characteristic for the $S \rightarrow C$ transition).^{11,24} When in its coiled or only weakly perturbed state, hydrodynamic interactions between chain segments play an important role (this state is called the Zimm limit), whereas they can be neglected in the fully extended state (freely draining or Rouse limit). A (geometric) prefactor should be included for the calculation of Zimm and Rouse relaxation times from λ_0 . However, both geometric prefactors are approximately equal to unity,¹¹ and we will not consider them further in this text. Since $\lambda_{Rouse} > \lambda_{Zimm}$, the critical extensional rate is higher for the $C \rightarrow S$

than for $S \rightarrow C$ transition (cf. eq 3), and hysteresis exists between both processes.

Relaxation Times of Polymer Chains in Dilute Solutions. The longest characteristic relaxation time λ_0 of a polymer chain in (dilute) solution can be determined by using viscometry since it is directly proportional to the limiting viscosity number $[\eta]_0$, which is a measure for the hydrodynamic volume of a polymer chain in solution.²⁵

$$\lambda_0 = [\eta]_0 \frac{\eta_s M}{RT} \quad (4)$$

In this equation, η_s is the viscosity of the solvent, M is the molecular weight of the polymer, R is the gas constant ($8.3145 \text{ J mol}^{-1} \text{ K}^{-1}$), and T is the absolute temperature. Often, the Mark–Houwink relation is used to relate the limiting viscosity number to the molecular weight M of a polymer chain:

$$[\eta]_0 = KM^a \quad (5)$$

The constants K and a are uniquely defined for each set of polymer and solvent. For numerous polymer–solvent pairs, values of K and a are tabulated in the literature and polymer handbooks. In addition, the value of the Mark–Houwink exponent a provides information about the solvent quality of a particular solvent for the polymer: for flexible polymers, a ranges from $1/2$ in a θ solvent (a solvent in which the polymer has no excluded volume effects and where it adopts a perfect random-coil conformation, obeying Gaussian chain statistics) to $4/5$ in a good solvent (where excluded volume effects play a role).²⁵

Alternatively, the limiting viscosity number can be determined experimentally by determining the specific viscosity η_{sp} of dilute polymer solutions having a known polymer concentration c . The limiting viscosity number is found by extrapolation of these data to the fictive situation of zero polymer concentration:²⁵

$$[\eta]_0 = \lim_{c \rightarrow 0} \frac{\eta_{sp}}{c} \quad (6)$$

Mechanochemical Bond Scission; Thermally Activated Barrier to Scission (TABS) Theory. For covalent bonds, mechanochemical bond scission is often treated according to the thermally activated barrier to scission (TABS) theory.^{5,10,26} TABS theory treats mechanochemical bond scission as being a thermally activated process. It states that the potential energy landscape of a chemical bond, as given by the Morse potential $U(r)$, is lowered under the influence of an external force, F_{ext} . This reduction is a result of the mechanical work that is put into the system by elongation of the chemical bond, and it results in a reduction of the bond dissociation energy D (see Figure 1).

The maximum force on the center of a (fully extended) polymer chain consisting of N statistical chain segment (each having a length b) can be calculated using the bead–rod model:^{9,11,20}

$$F_{\text{max}} = \frac{3\pi}{4} \eta_s a b \epsilon S N^2 \quad (7)$$

Here η_s is the viscosity of the solvent, a is the radius of a bead, $\epsilon = dv_x/dx$ is the strain rate (equal to the velocity gradient) in solution as a result of distortions in the flow pattern, and S is the so-called “shielding factor” that accounts for hydrodynamic interactions between beads. When a polymer chain is fully extended, these interactions can be neglected and S is often set equal to 1. Since the number of statistical chain segments scales

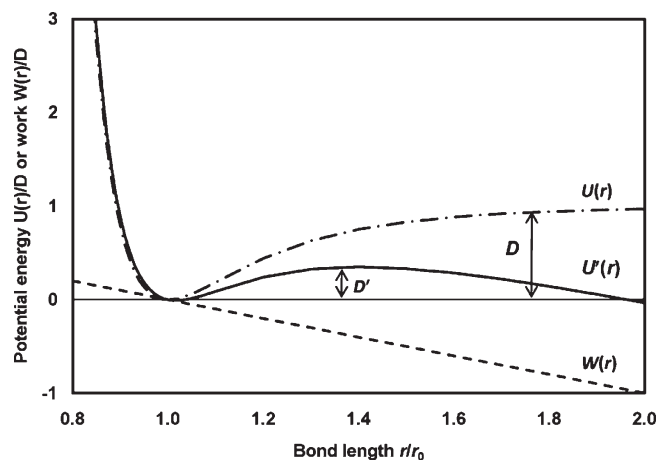


Figure 1. Morse energy potentials representing a chemical bond in unperturbed state (dash-dotted line) and of a bond under stress (solid line) showing the mechanochemical activation of bond according to the TABS theory. The energy input due to mechanical work is shown as a dashed line.

proportionally to the molecular weight of the polymer chain, it can be deduced that $F_{\text{ext}} \propto M^2$.

In thermal activation, the energy barrier for scission is overcome by heating the system in order to increase its internal energy. For mechanochemical activation, TABS theory dictates that mechanochemical scission will occur when the external force is high enough to reduce the dissociation energy to a value D' which is in the order of the thermal energy of the atoms, i.e., several times $k_B T$ (with the Boltzmann constant $k_B = 1.38 \times 10^{-23} \text{ J K}^{-1}$). In that case, thermal fluctuations which are typically in the order of several $k_B T$ ($k_B T \approx 2.4 \text{ kJ mol}^{-1}$ at 25°C) around the equilibrium position are sufficient to overcome the energy barrier D' .

EXPERIMENTAL SECTION

Synthesis of α -(*N*-ethylimidazolium)- ω -methoxy Poly-(tetrahydrofuran) Polymers. Polymers NHC_x (with x being the approximate M_n of the polymer ligand) were synthesized via cationic ring-opening polymerization of tetrahydrofuran (THF) using methyl triflate as initiator (see Figure 2).²⁷ The polymerization was terminated with ca. 2 equiv of *N*-ethylimidazole. Ion exchange, first using DOWEX chloride ion-exchange resin and subsequently ammonium hexafluorophosphate (NH_4PF_6) were carried in methanol out using the same procedure as reported in earlier work.^{1,21} After complete work-up the resulting polymer was characterized by ^1H NMR and gel permeation chromatography (GPC). The results of the characterization are summarized in Table 1. For a more detailed experimental procedure, see the Supporting Information.

Synthesis of Silver(I)–NHC Polymer Complexes $\text{Ag}(\text{NHC}_x)_2\text{PF}_6$. Complexation of polymers NHC_x with silver(I) was typically performed by stirring the polymers in dichloromethane in the presence of excess silver(I) oxide and a small amount of aqueous 1 M NaOH solution for 1–2 days (see Figure 2).²¹ After complete work-up, complexation with silver(I) was confirmed by ^1H NMR. For a more detailed experimental procedure, see the Supporting Information.

Gel Permeation Chromatography. Gel permeation chromatography (GPC) of polymers NHC_x was performed on a PL-GPC 50 Plus system (Polymer Laboratories) using DMF/LiBr (10 mM) as eluents with the integrated refractometer for detection. A typical single run was carried out at 50°C and took 15 min at a liquid flow rate of

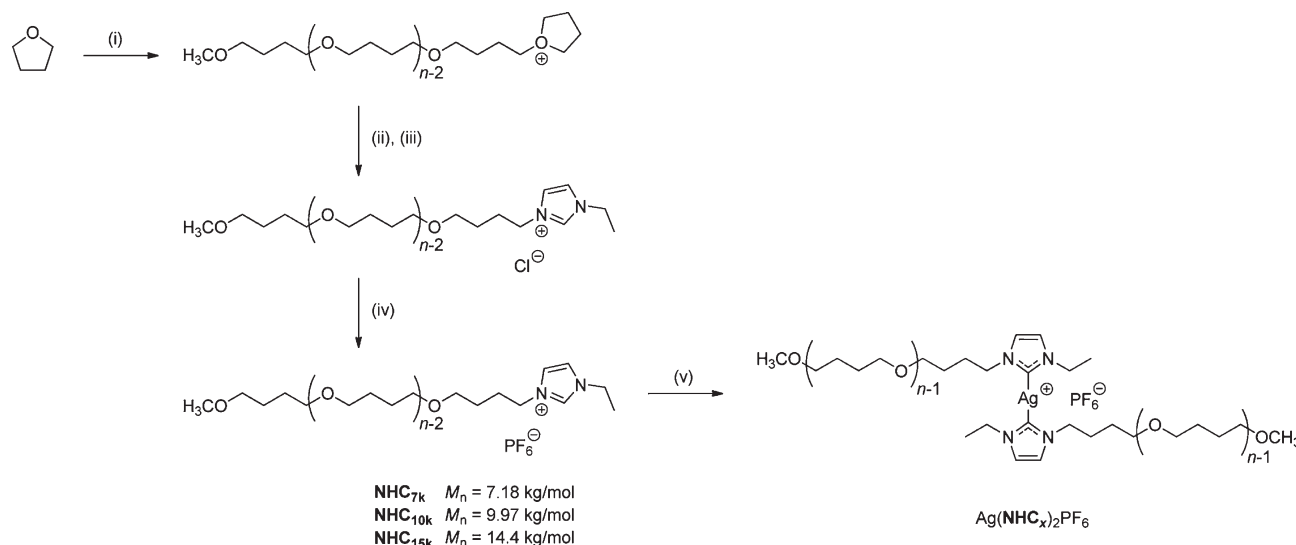


Figure 2. Reaction scheme for the polymerization and complexation reactions for the synthesis of polymer complexes $\text{Ag}(\text{NHC}_x)_2\text{PF}_6$ starting from the cationic ring-opening polymerization of THF. Reaction conditions: (i) methyl triflate and di-*tert*-butylpyridine, Ar, 0 °C, 3–6 h; (ii) 2 equiv of *N*-ethylimidazole, Ar, 0 °C, 30 min; (iii) DOWEX ion-exchange resin, CH_3OH , rt, 2 h; (iv) NH_4PF_6 , CH_3OH , rt, 2 h; (v) excess Ag_2O , CH_2Cl_2 /1 M NaOH solution, rt, 1–2 days.

Table 1. Summary of the Characteristics of Polymers NHC_x That Were Synthesized and Used in This Study

polymer	end group	counterion	determined M_n (kg mol^{-1})	
			GPC ^a	¹ H NMR
$\text{NHC}_{7\text{K}}$	<i>N</i> -ethylimidazolium	PF_6^-	7.18 (1.11)	7.82
$\text{NHC}_{10\text{K}}$	<i>N</i> -ethylimidazolium	PF_6^-	9.97 (1.10)	11.7
$\text{NHC}_{15\text{K}}$	<i>N</i> -ethylimidazolium	PF_6^-	14.4 (1.16)	15.0

^a Values of the polydispersity index ($\text{PDI} = M_w/M_n$) are shown in parentheses. All values are determined versus poly(ethylene oxide) standards using DMF/LiBr as eluents.

1 mL/min. The number- and weight-average molecular weights were obtained versus poly(ethylene oxide) standards. Comparison between these values and the value of the number-average molecular weight obtained from end-group analysis in ¹H NMR showed very good agreement (Table 1).

Viscosity Measurements. Ubbelohde viscosity measurements were carried out using a capillary viscometer (manufactured by Schott Instruments, Germany; i.d. 0.40 mm). For temperature control, the glass capillary was immersed in a thermostat bath (Schott Instruments CT52, by Schott Instruments, Germany) equilibrated at 28.00 ± 0.02 °C. For the viscosity measurements, solutions were prepared containing between 2.5 and 12.5 mg mL^{-1} of polymer complexes $\text{Ag}(\text{NHC}_x)_2\text{PF}_6$ in toluene. The specific viscosities of these polymer solutions were calculated by comparing their elution times Δt with that of the pure solvent as reference Δt_s according to

$$\eta_{\text{sp}} = \frac{\eta - \eta_s}{\eta_s} \approx \frac{\Delta t - \Delta t_s}{\Delta t_s} \quad (8)$$

Strictly speaking, eq 8 is only valid when the density of the polymer solution is approximately the same as the density of the pure solvent i.e., under dilute solution conditions. For all experiments in this work it was confirmed that this criterion was fulfilled.

Molecular Dynamics Simulations. To gain an atomistic insight in the response of the silver(I)–NHC bond to external force, *ab initio* molecular dynamics (*ab initio* MD) simulations were performed on this

system.²⁸ The system has been initially optimized using the SIESTA code.²⁹ GGA approximation has been applied, with PBE functional describing the exchange-correlation term. DZP basis set shipped together with SIESTA has been used. The same parameters have been used for all subsequent calculations. The system has been put into a 30 Å cubic periodic box to provide enough space to stretch and to prevent the interaction of the system with its periodic images in neighboring boxes. The artificial force was acting on the two hydrogen atoms in the opposite directions, along the arbitrarily selected axis.

After initial optimization of the system, the optimized geometries were used as initial geometries for the NVT MD runs. The runs lasted for 20 000 steps with a time step of 0.5 fs resulting in a total simulated time period of 10 ps. The time step was short enough to ensure the system was simulated properly as is evident by the conservation of the energy of the system during the run and the smooth motion of atoms. Temperature was set at 298 K, and it was controlled by a Nose thermostat. We have carried out five *ab initio* MD simulations, with the magnitude of the artificial force increasing from 0.4 to 2.0 nN.

In addition, constrained geometry optimization calculations in the presence of an artificial force acting on the molecular model were carried out using the same initial geometry of the system. These optimization provide us with the potential energy surfaces similar to those obtained by the groups of Moore,¹⁷ Martínez,¹⁸ and Marx^{30,31} to study e.g. the mechanochemical ring-opening of benzocyclobutanes. The constraint put upon the system was a fixed distance between the Ag and C2 atoms (i.e., the length of the silver(I)–NHC coordination bond). A series of constrained geometry optimizations were carried out with the C2–Ag distance varying from 2.0 to 4.0 Å with steps of 0.2 Å. These simulations allowed determining the influence of the external force on the activation barrier for the dissociation of the Ag–C2 coordination bond. The bond cleavage is possible when the work done by the external force overcomes the increase of the system's potential energy along the reaction coordinate.

RESULTS AND DISCUSSION

Synthesis of Polymers NHC_x and Their Corresponding Supramolecular Polymer Complexes. To study the physical aspects of mechanochemical chain scission of supramolecular polymers in solution, supramolecular polymer complexes

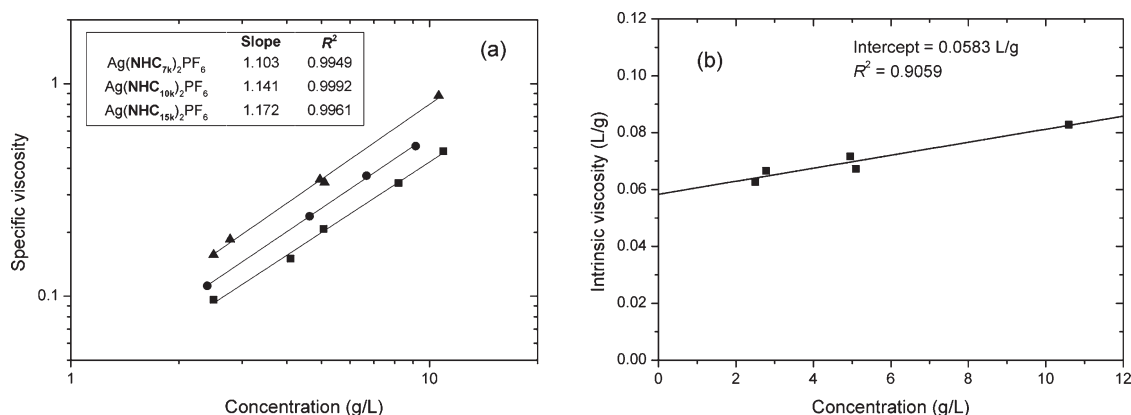


Figure 3. (a) Specific viscosity η_{sp} of the polymer complex solutions as a function of polymer concentration c in toluene at 28.00 ± 0.02 °C: (■) $\text{Ag}(\text{NHC}_{7K})_2\text{PF}_6$; (●) $\text{Ag}(\text{NHC}_{10K})_2\text{PF}_6$ and (▲) $\text{Ag}(\text{NHC}_{15K})_2\text{PF}_6$. (b) Intrinsic viscosity of solutions of $\text{Ag}(\text{NHC}_{15K})_2\text{PF}_6$ in toluene. The solid line represents the best linear fit of the data.

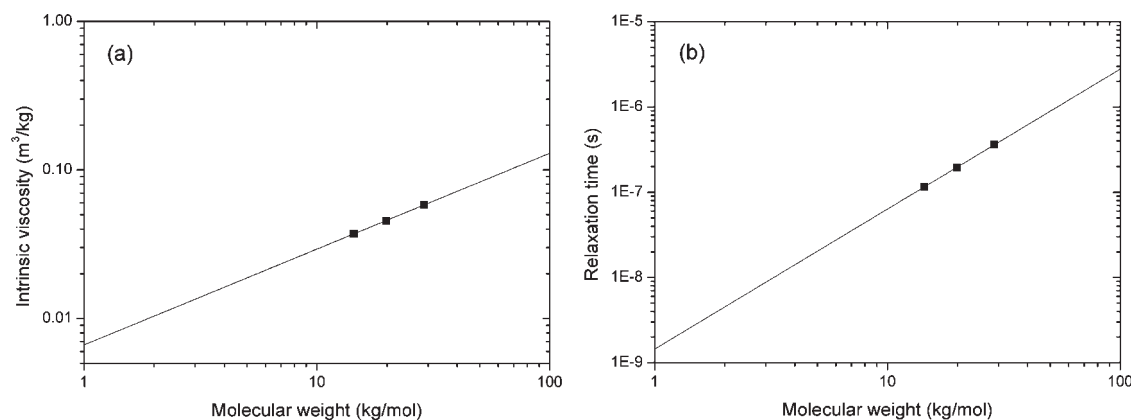


Figure 4. (a) Mark–Houwink plot and (b) relaxation times for the supramolecular polymer complexes $\text{Ag}(\text{NHC}_x)_2\text{PF}_6$. The solid line represents the best fit of the experimental data.

$\text{Ag}(\text{NHC}_x)_2\text{PF}_6$ were synthesized. The synthetic route toward the supramolecular complexes, starting with the cationic ring-opening polymerization of THF, is shown in Figure 2. Table 1 summarizes the results of full characterization of polymers NHC_x . A more detailed description of the synthetic procedure and characterization methods of these polymers and their corresponding supramolecular polymer complexes is given in the Supporting Information. The M_n values obtained by GPC agree well with those obtained by ^1H NMR, which is a clear indication of successful end-group functionalization.

Kinetics of Ultrasound-Induced Silver(I)–NHC Polymer Chain Scission. Ultrasound-induced chain scission kinetics of $\text{Ag}(\text{NHC}_x)_2\text{PF}_6$ polymers could not be monitored by GPC. When analyzed with a chloroform mobile phase, broad and ill-defined peaks were observed for the imidazolium ligands, possibly owing to ionic aggregation and interactions of the polar end groups with the column. When DMF, a more polar mobile phase, was used to suppress aggregation, hydrolysis of the silver(I)–NHC complexes took place, and all polymeric material eluted from the column as uncomplexed imidazolium salts.

Relaxation Times of Silver(I)–NHC Polymer Complexes in Dilute Solutions. Ubbelohde capillary viscometry was used to determine the relative viscosities of solutions of the supramolecular polymer complexes $\text{Ag}(\text{NHC}_x)_2\text{PF}_6$ in toluene at 28.00 ± 0.02 °C.³²

By plotting the specific viscosity of the solutions of these polymer complexes in toluene versus polymer complex concentration (as shown in Figure 3a), it was confirmed that all solutions could be considered as dilute since the slopes of the obtained lines are almost equal to unity.

Equation 6 was used to determine the limiting viscosity number $[\eta]_0$ from these data. The values of η_{sp}/c were plotted versus polymer concentration c on a double-logarithmic scale (the graph for complex $\text{Ag}(\text{NHC}_{15K})_2\text{PF}_6$ is given as an example in Figure 3b; for the graphs of the other complexes, see Supporting Information). As expected, all data points fall approximately onto a straight line that was extrapolated to $c \rightarrow 0$ by linear regression to determine $[\eta]_0$.

Mark–Houwink parameters for the silver(I)–NHC polymer complexes were determined from the slope and abscissa of a double-logarithmic plot of the obtained values for $[\eta]_0$ versus the number-average molecular weight M_n as determined from GPC measurements (see Figure 4a). Linear regression shows that $a = 0.65$ and $\log(K) = -2.18$ (i.e., $K = 6.6 \times 10^{-3}$ L/g). Even though these values should be treated as rough estimates which are based on only a small data set, they are consistent with literature, where values of a ranging between 0.59 and 0.78 are reported for covalent PTHF in toluene.^{32,33} The precise value of a depends on the range of molecular weights and the polydispersity of the

Table 2. Limiting Viscosity Numbers, Longest Characteristic Relaxation Times, and Critical Strain Rates for Coil-to-Stretch Transition for the Ag(NHC_x)₂PF₆ Complexes in This Study

complex	M_n (kg mol ⁻¹) ^a	$[\eta]_0$ (L g ⁻¹) ^b	λ_0 (s)	$\dot{\epsilon}_{\text{crit}}$ (s ⁻¹)
Ag(NHC _{7K}) ₂ PF ₆	14.4	0.0373	1.2×10^{-7}	4.3×10^6
Ag(NHC _{10K}) ₂ PF ₆	19.9	0.0453	2.0×10^{-7}	2.6×10^6
Ag(NHC _{15K}) ₂ PF ₆	28.8	0.0583	3.6×10^{-7}	1.4×10^6

^a Calculated as twice the M_n of each polymer ligand according to GPC (see Table 1). ^b Experimental value, as obtained from Ubbelohde viscometry.

polymer samples that were used to determine the Mark–Houwink parameters and the temperature at which the experiments were carried out.^{32–34} In conclusion, it is clear that toluene is a good solvent for PTHF and the analogous polymer silver(I)–NHC complexes, indicated by the fact that $a > 1/2$ in this study and in all cases reported in the literature.

The longest characteristic relaxation time λ_0 of the polymer complex chains is calculated from these data using eq 4. The results of all the calculations are summarized in Table 2. It is observed that the longest characteristic relaxation times λ_0 for the polymer complexes used in this study and in previous work are in the order of several tenths of microseconds ($\sim 10^{-7}$ s) and that they scale with molecular weight as $\lambda_0 \propto M_n^{1.64}$ (Figure 4b).

Estimation of the Critical Extensional Rate for Coil-to-Stretch Transition. For the silver(I)–NHC polymer complexes studied in this work, the longest characteristic relaxation times of the polymer chains as a function of total molecular weight were determined. It was shown that for the typical molecular weights that have been used in this and previous work ($M_n = 10$ – 40 kg mol⁻¹) these relaxation times are in the order of 0.1 – 0.5 μ s (1×10^{-7} – 5×10^{-7} s). With these results, the critical strain rates in solution $\dot{\epsilon}_{\text{crit}}$ can be calculated (i.e., the strain rates that are typically required to obtain coil-to-stretch transition of the polymer complex chains). By applying the criterion of the critical Deborah number, as formulated in eqs 3 and 4, it is found that $\dot{\epsilon}_{\text{crit}} \sim 10^6$ – 10^7 s⁻¹. The values of $\dot{\epsilon}_{\text{crit}}$ have been included with Table 2.

In our previous work, numerical simulations of the cavitation process in toluene were performed,²¹ taking in account the typical conditions of scission experiments. It was shown that strain rates as high as $\sim 10^8$ s⁻¹ were reached during the first collapse event of a cavitation bubble; in addition, strain rates remained higher than $\sim 10^6$ s⁻¹ for the subsequent four to five collapses (“bounces”). On the basis of the simulations and the findings in this work, it can be concluded that the strain rates typically obtained in ultrasound experiments are sufficient for coil-to-stretch transition of the silver(I)–NHC polymer complexes in solution to occur.

Now since the first step in mechanochemical scission of polymer chains, being the coil-to-stretch transition, is apparently not significantly altered when going from a covalent to an analogous supramolecular polymer, it seems obvious that the introduction of a metal–ligand coordination bond in the center of the polymer chain is solely responsible for lowering the limiting molecular weight for mechanochemical scission. In terms of the TABS theory, the weaker metal–ligand coordination bond in the supramolecular polymer has a lower energy potential at rest (hence a lower dissociation energy D); therefore, when compared to covalent bonds in a polymer backbone

(typically C–C and or C–O bonds which have bond energies around 350 kJ mol⁻¹), less mechanical work is required for the bond to lower its dissociation energy to $D' \sim k_B T$. This means that (cf. eq 7) a polymer chain consisting of less statistical segments N (i.e., a shorter polymer chain) is already sufficient to transduce the required force on the central bond.

Potential Energy Diagram for Ag–C Bonds under External Force. In the previous sections we have demonstrated that the strain rates required to achieve coil-to-stretch transition of the polymer catalyst complexes considered is in the order of 10^6 – 10^7 s⁻¹. After extension of the polymer chain, mechanical forces accumulate along the (contour) length of the polymer chain. These forces are transmitted from the solvent to the polymer chain through viscous coupling as described by the bead–rod model (see eq 7). The crucial question to be answered at this stage is whether or not the accumulated forces are enough to cleave the Ag–C bond.

Two series of simulations have been carried in order to answer this question. First was the molecular dynamics (MD) simulation, which allowed us to gain insight into the cleavage phenomenon. On the basis of their relative bond strengths, the coordination bond is expected to break easier than the covalent bonds; hence, it was assumed that the Ag–C bond is the place where scission would occur. MD simulations combined with the steering force could confirm that assumption. However, because the time scale of the MD simulations and the experiments differ by several orders of magnitude, the accuracy of the assessment of the rupture force is not accurate in this case.

Therefore, a second series of simulations were carried out, using constrained geometry optimizations (COGEF), where the constraint was identical to that of the MD simulations. The exact details of the computational procedure are listed in the Experimental Section. The optimized model is shown in the top left of Figure 5. The central Ag atom is coordinated by two carbon atoms (marked as C1 and C2) that belong to two imidazolium rings. The ethyl groups attached to the rings are the simplified model of the long chain polymer chains that transfer the external force to the central coordination bond. It has been recently reported by Marx et al.³¹ that the length of the side chains is important for the correct assessment of the mechanochemical properties of covalent polymers. They demonstrated that in the case of a benzocyclobutane core functionalized with polyethylene (PE) chains the angle between the side chains and the benzocyclobutane moiety (the angle being determined by the length of the PE chain) is the main factor affecting the accuracy of the predicted values of the rupture force. However, because of the much higher flexibility and the coordination nature of bonding within our model as compared to the covalent polymer considered by Marx et al., this factor is expected to be only minor in the case considered here. Therefore, the use of the simplified 1-ethyl-3-methylimidazolium ligands is justified for the purpose of the present study.

In the *ab initio* MD simulations an initial reorganization of the geometry with respect to the external force is observed, after which the system stabilizes with deformed geometry. The local geometrical deformation observed within the complex depends on the forces acting on hydrogen atoms. In the equilibrium state (without external force acting) the bond length equals 2.06 Å. Under an external force, the average bond length between the Ag and C2 atoms increases from 2.10 Å at $F_{\text{ext}} = 0.4$ nN, to 2.13 Å (0.8 nN), 2.16 Å (1.2 nN), and reaches 2.22 Å at $F_{\text{ext}} = 1.6$ nN (Figure 5). When an external force of 2.0 nN is applied, the

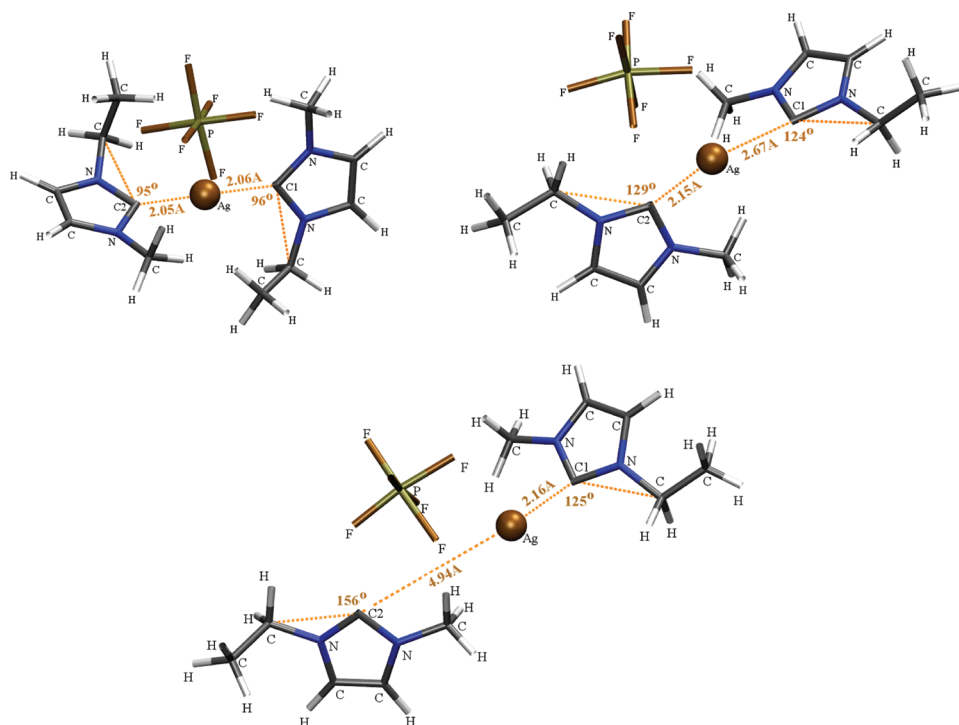


Figure 5. Stages of bond cleavage in MD simulation with an artificial force of 2.0 nN. Top left: initial structure with relaxed coordinates. Top right: stretched conformation as a result of force acting on hydrogen atoms. Bottom: structure after the Ag–C bond cleavage, with one of the NHC ligands separated from the complex.

cleavage of the Ag–C bond is observed within the 10 ps time scale of the MD run.

COGEF analysis provides more insight into the impact of the external force on the mechanochemical scission of the polymer silver(I)–NHC complexes. The potential energy surfaces corresponding to the cleavage of Ag–C bond under increasing external force was analyzed. After the initial preoptimization of the complex in absence of geometrical constraints, another geometry optimization was carried out with an external force of 1.0 nN to reorient the system with respect to the external force, as observed in the MD simulations. Subsequently, the geometry was optimized further in the absence of geometrical constraints, but with the complex aligned within the periodic box in such a way as if there were still external forces applied. The geometry obtained at this stage was used as the initial geometry for the constrained optimization procedure.

Seven series of constrained geometry optimization simulations were performed with a gradually increasing external force varying between 82 and 823 pN. Moreover, as a reference, we have carried out one simulation without external force. The energy change upon the increase of Ag–C bond length was monitored for each of the values of external force. The Ag–C distance was initially set to 2.0 Å and was increased to the value of 4.0 Å with steps of 0.1 Å. At each step total energy has been calculated, and the work done by the external force has been evaluated from the equation $W = F_{\text{ext}}\Delta x$, where W is the work done by the force, F_{ext} is the external force acting on the atoms, and Δx is the displacement of these atoms from their optimal position along the direction of the external force. This procedure resulted in the reaction energy diagrams for the mechanochemical activation of a silver(I)–NHC complex under the influence of the increasing external force (Figure 6). When no external force is applied, the

energy barrier for the Ag–C bond cleavage is just above 2 eV ($\sim 200 \text{ kJ mol}^{-1}$), which is in close agreement with bond energies found in the literature³⁶ and indeed much lower than bond dissociation energies for C–C and C–O bonds (both around 350 kJ mol^{-1}). The activation barrier decreases gradually with increasing force until it finally disappears at the external force of 823 pN. It is also noticed that the maximum energy shifts toward shorter bond lengths upon increasing force.

We may now speculate on the magnitude of the force necessary to break the Ag–C bond in the investigated system. From the MD calculations it turns out that a force of 2.0 nN is sufficient to break the Ag–C bond at the very early stage, even before the system stabilizes. Already the first pull caused by the external force is sufficient to overcome the energy barrier. In the simulation with the force of 1.6 nN applied, we can observe that the system remains intact during the run; hence, we can conclude that the force necessary to readily break the Ag–C bond would be in between 1.6 and 2.0 nN. This calculated value is close to the experimentally observed force for bond cleavage in similar systems applying a force of less than 1 nN. The COGEF simulations show a better agreement with the experiment. A low-energy barrier (around 0.2 eV or 20 kJ mol^{-1}) is observed in the presence of an external force of 412 pN, and the barrier has completely disappeared for a force of 823 pN. However, the small energy barrier that is still present at a force of 412 pN can still be overcome by thermal fluctuations on time scales typical for ultrasound experiments (which are in the order of 10^{-6} s). Therefore, based on the potential energy diagram in Figure 6, the value for the force required to break silver(I)–NHC coordination bonds can be estimated to be between 400 and 500 pN.

This discrepancy between the MD and COGEF simulations can be explained by the time scale of the simulation with respect

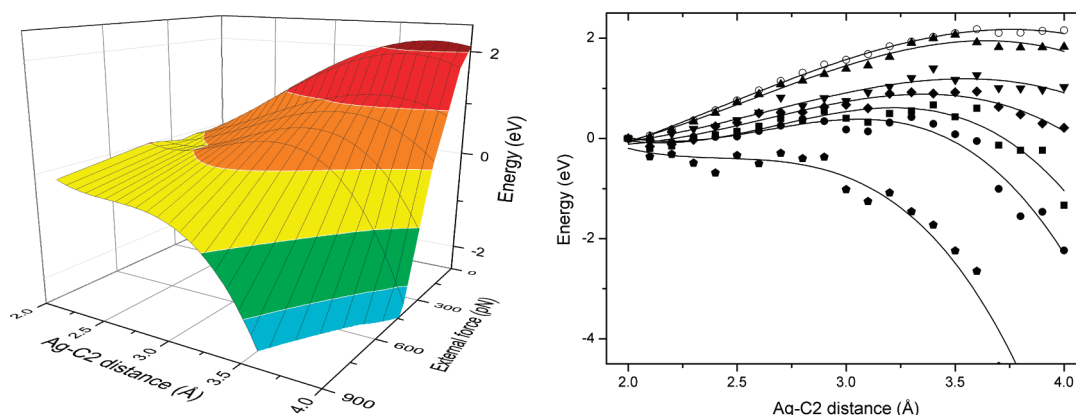


Figure 6. Left: the potential energy surface of the Ag–C bond cleavage under the external force. Right: the potential energy diagrams at various selected external forces: (○) no external force, (▲) 82 nN, (▼) 165 nN, (◆) 247 nN, (■) 329 nN, (●) 412 nN, and (●) 823 nN.

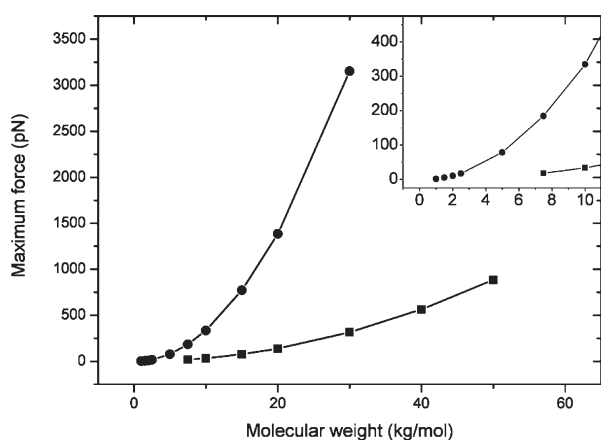


Figure 7. Maximum force (in pN) on fully extended polymer chains as a function of molecular weight (kg mol^{-1}) at typical strain rates of 10^7 s^{-1} (■) and 10^8 s^{-1} (●).

to the experiment. As we mentioned before, we have simulated only 10 ps of the life of the system, whereas $1 \mu\text{s}$ is the time scale of the experiment. Literature sources provide some more details on the value of the force versus time scale for different types of bonds.^{5,37} Although there is no Ag–C type of bond mentioned in the reference, we may assume that the trend will be continued, and we could expect the force to be lowered by approximately 15–25%. This value is even closer to the experiment, despite the simplifications used in our model such as the shorter aliphatic chains at the N1 position of the NHC ligands and absence of the solvent.

The maximum force F_{ext} on polymer chains as a function of increasing molecular weight is shown in Figure 7 for typical strain rates $\epsilon = 10^7$ and 10^8 s^{-1} .²¹ These values are rough estimates calculated based on the bead–rod model³⁸ as given by eq 7. From these calculations, we would expect M_{lim} for the polymer silver(I)–NHC complexes to be around 30 kg mol^{-1} for $\epsilon = 10^7 \text{ s}^{-1}$ and between 10 and 15 kg mol^{-1} for $\epsilon = 10^8 \text{ s}^{-1}$, respectively. Taking in account the fact they are only rough estimates, these values are in good agreement with previous experimental observations. Furthermore, these values indicate that purely mechanochemical bond scission is possible under ultrasound conditions without the aid of any chemical process that would facilitate bond scission (chemically facilitated scission). So, even

though the contribution of chemically facilitated mechanochemical bond scission is not excluded based on the present results, it can be concluded that its presence is not an absolute requirement to explain the high observed scission efficiency at molecular weight below M_{lim} of covalent PTHF.

CONCLUSIONS

In the present study, we studied the unfolding and mechanochemical scission of silver(I)–NHC supramolecular polymer complexes. It was confirmed that both (unperturbed) polymer chain dimension as well as the critical strain rate for coil-to-stretch transition is similar for both the supramolecular polymer and its fully covalent analogue, irrespective of the presence of the coordination complex within the polymer chain. On the basis of the results from earlier numerical simulations of the cavitation process in ultrasound,²¹ it was concluded that coil-to-stretch transition is in fact expected to occur readily for these supramolecular polymers, even though their molecular weight is relatively low (well below M_{lim} for covalent PTHF, see ref 4).

In addition, molecular dynamic (MD) simulations, combined with COGEF analysis, resulted in a potential energy diagram for Ag–C bonds under external force. From this potential energy diagram it became clear that application of an external force of 400–500 pN would be sufficient to achieve scission of the Ag–C bonds at room temperature. During none of the performed MD simulations, scission of a covalent bond within the systems was observed. The obtained force for mechanochemical chain scission is about 1 order of magnitude lower than the forces typically required to break covalent bonds in polymer chains (in the literature, for C–C bonds values ranging between 2 and 13 nN are found).^{5,9}

Taking all these results into account, it is confirmed that the reduction of M_{lim} in supramolecular polymers is due to the incorporation of the metal–ligand coordination bond within the polymer backbone. Such a metal–ligand coordination bond is significantly weaker ($D \approx 200 \text{ kJ mol}^{-1}$ for Ag–C bonds) than typical covalent bonds, such as C–C and C–O bonds that make up the polymer backbone ($D \approx 350 \text{ kJ mol}^{-1}$). As a result of the weaker bond, a lower force is required to reduce the energy barrier for bond scission to a value that is readily overcome by thermal fluctuations at ambient temperature (as dictated by TABS theory). Radical-induced chain scission can be excluded as a predominant mechanism based on findings in previous

work,²¹ and the possible role of chemically facilitated mechanochemical chain scission was evaluated here. A possible facilitating mechanism consists of reduction of the dissociation energy barrier by activation of the Ag–C bond in the transition state of the cleavage process. Even though the occurrence of chemically facilitating mechanisms cannot be excluded, it is confirmed that such a mechanism is definitely not a prerequisite for chain scission of these supramolecular polymers using ultrasound. Since the Ag–C bond in the silver(I)–NHC coordination complex is several times weaker than a covalent bond, the prevalent conditions in ultrasound experiments allow for purely mechanochemical bond scission.

■ ASSOCIATED CONTENT

S Supporting Information. Full details of the synthetic procedures and characterization data of the polymers and their corresponding supramolecular polymer complexes as well as data of the viscosity measurements. This material is available free of charge via the Internet at <http://pubs.acs.org>.

■ AUTHOR INFORMATION

Corresponding Author

*E-mail: r.p.sijbesma@tue.nl.

■ ACKNOWLEDGMENT

The authors gratefully acknowledge financial support from the Dutch National Research School Combination Catalysis Controlled by Chemical Design (NRSC-Catalysis). NWO-NCF (SH-170-11) is gratefully acknowledged for providing access to supercomputer facilities.

■ REFERENCES

- (1) Karthikeyan, S.; Potisek, S. L.; Piermattei, A.; Sijbesma, R. P. *J. Am. Chem. Soc.* **2008**, *130*, 14968–14969.
- (2) Piermattei, A.; Karthikeyan, S.; Sijbesma, R. P. *Nature Chem.* **2009**, *1*, 133–137.
- (3) Tennyson, A. G.; Wiggins, K. M.; Bielawski, C. W. *J. Am. Chem. Soc.* **2010**, *132*, 16631–16636.
- (4) Paulusse, J. M. J. Reversible Mechanochemistry of Coordination Polymers and Networks. PhD Thesis, Eindhoven University of Technology, Eindhoven, The Netherlands, 2006.
- (5) (a) Beyer, M. K. *J. Chem. Phys.* **2000**, *112*, 7307–7312. (b) Beyer, M. K.; Clausen-Schaumann, H. *Chem. Rev.* **2005**, *105*, 2921–2948.
- (6) Staudinger, H.; Heuer, W. *Ber. Deutsch. Chem. Ges.* **1934**, *67*, 1159–1164.
- (7) Basedow, A. M.; Ebert, K. H. *Adv. Polym. Sci.* **1977**, *22*, 83–148.
- (8) (a) Porter, R. S.; Johnson, J. F. *J. Phys. Chem.* **1959**, *63*, 202–205. (b) Merrill, E. W.; Leopairat, P. *Polym. Eng. Sci.* **1980**, *20*, 505–511. (c) Dunlap, P. N.; Leal, L. G. *J. Non-Newtonian Fluid Mech.* **1987**, *23*, 5–48. (d) Clay, J. D.; Koelling, K. W. *Polym. Eng. Sci.* **1997**, *37*, 789–800. (e) Kang, K.; Lee, L. J.; Koelling, K. W. *Exp. Fluids* **2005**, *38*, 222–232.
- (9) (a) Muller, A. J.; Odell, J. A.; Carrington, S. *Polymer* **1992**, *33*, 2598–2604. (b) Odell, J. A.; Keller, A. *J. Polym. Sci., Part B: Polym. Phys.* **1986**, *24*, 1889–1916.
- (10) Odell, J. A.; Keller, A.; Muller, A. J. *Colloid Polym. Sci.* **1992**, *270*, 307–324.
- (11) Nguyen, T. Q.; Kausch, H.-H. *Adv. Polym. Sci.* **1992**, *100*, 73–184.
- (12) Typically, for covalent polymers the value for M_{lim} is between 40 and 100 kg mol⁻¹, see e.g. refs 4, 8a, 8d, 9b, 20, and Price, G. J.; Smith, P. F. *Polymer* **1993**, *34*, 4111–4117.
- (13) Encina, M. V.; Lissi, E.; Sarasua, M.; Gargallo, L.; Radic, D. *J. Polym. Sci., Polym. Lett. Ed.* **1980**, *18*, 757–760.
- (14) Berkowski, K. L.; Potisek, S. L.; Hickenboth, C. R.; Moore, J. S. *Macromolecules* **2005**, *38*, 8975–8978.
- (15) Davis, D. A.; Hamilton, A.; Yang, J.; Cremer, L. D.; Van Gough, D.; Potisek, S. L.; Ong, M. T.; Braun, P. V.; Martínez, T. J.; White, S. R.; Moore, J. S.; Sottos, N. R. *Nature* **2009**, *459*, 68–72.
- (16) Wu, D.; Lenhardt, J. M.; Black, A. L.; Akhremitchev, B. B.; Craig, S. L. *J. Am. Chem. Soc.* **2010**, *132*, 15936–15938.
- (17) Hickenboth, C. R.; Moore, J. S.; White, S. R.; Sottos, N. R.; Baudry, J.; Wilson, S. R. *Nature* **2007**, *446*, 423–427.
- (18) Ong, M. T.; Leiding, J.; Tao, H.; Virshup, A. M.; Martínez, T. J. *J. Am. Chem. Soc.* **2009**, *131*, 6377–6379.
- (19) Black, A. L.; Orlicki, J. A.; Craig, S. L. *J. Mater. Chem.* **2011**, *21*, 8460–8465.
- (20) Kuipers, M. W. A.; Iedema, P. D.; Kemmere, M. F.; Keurentjes, J. T. F. *Polymer* **2004**, *45*, 6461–6467.
- (21) Rooze, J.; Groote, R.; Jakobs, R. T. M.; Sijbesma, R. P.; Van Iersel, M. M.; Rebrov, E. V.; Schouten, J. C.; Keurentjes, J. T. F. *J. Phys. Chem. B* **2011**, *115*, 11038–11043.
- (22) (a) Ballauff, M.; Wolf, B. A. *Macromolecules* **1984**, *17*, 209–216. (b) Bueche, F. *J. Appl. Polym. Sci.* **1960**, *4*, 101–106. (c) Price, G. J.; West, P. J.; Smith, P. F. *Ultrason. Sonochem.* **1994**, *1*, S51–S57.
- (23) (a) Smith, D. E.; Chu, S. *Science* **1998**, *281*, 1335–1340. (b) Dyakonova, N. E.; Odell, J. A.; Brestkin, Y. V.; Lyulin, A. V.; Saez, A. E. *J. Non-Newtonian Fluid Mech.* **1996**, *67*, 285–310. (c) De Gennes, P. G. *J. Chem. Phys.* **1974**, *60*, 5030–5042.
- (24) Larson, R. G.; Magda, J. J. *Macromolecules* **1989**, *22*, 3004–3010.
- (25) Larson, R. G. In *Constitutive Equations for Polymer Melts and Solutions*; Butterworths: New York, 1988.
- (26) Zhurkov, S. N.; Korsukov, V. E. *J. Polym. Sci., Phys. Ed.* **1974**, *12*, 385–398.
- (27) Dubreuil, M. F.; Farcy, N. G.; Goethals, E. J. *Macromol. Rapid Commun.* **1999**, *20*, 383–386.
- (28) Szyja, B. M.; Pidko, E. A.; Groote, R.; Hensen, E. J. M.; Sijbesma, R. P. *Proc. Comp. Sci.* **2011**, *4*, 1167–1176.
- (29) (a) Ordejón, P.; Artacho, E.; Soler, J. M. *Phys. Rev. B* **1996**, *53*, 10441–10444. (b) Soler, J. M.; Artacho, E.; Gale, J. D.; Garcia, A.; Junquera, J.; Ordejón, P.; Sánchez-Portal, D. *J. Phys.: Condens. Matter* **2002**, *14*, 2745–2779.
- (30) Ribas-Arino, J.; Shiga, M.; Marx, D. *Chem.—Eur. J.* **2009**, *15*, 13331–13335.
- (31) Ribas-Arino, J.; Shiga, M.; Marx, D. *J. Am. Chem. Soc.* **2010**, *132*, 10609–10614.
- (32) Evans, J. M.; Huglin, M. B. *Makromol. Chem.* **1969**, *127*, 141–152.
- (33) (a) Kurata, M.; Utiyama, H.; Kamada, K. *Makromol. Chem.* **1965**, *88*, 281–293. (b) Ali, S. A. M.; Hourston, D. J. *Eur. Polym. J.* **1993**, *29*, 783–789.
- (34) Dreyfuss, P. In *Poly(tetrahydrofuran)*; Gordon and Breach Science Publishers: New York, 1982.
- (35) Lenhardt, J. M.; Ong, M. T.; Choe, R.; Evenhuis, C. R.; Martínez, T. J.; Craig, S. L. *Science* **2010**, *329*, 1057–1060.
- (36) (a) Hu, X.; Castro-Rodriguez, I.; Olsen, K.; Meyer, K. *Organometallics* **2004**, *23*, 755–764. (b) Nemcsok, D.; Wichmann, K.; Frenking, G. *Organometallics* **2004**, *23*, 3640–3646.
- (37) Mendoza, J. P. M.; Valenzuela, O. E. A.; Flores, V. C.; Aquino, J. M.; De la Torre, A. D. *J. Alloys Compd.* **2004**, *369*, 144–147.
- (38) For calculation of F_{max} the following values have been used for the parameters in eq 7: $\eta_s = 5.6 \times 10^{-4}$ Pa s (viscosity of toluene at 25 °C; Santos, F. J. V.; et al. *J. Phys. Chem. Ref. Data* **2006**, *35*, 1–8.); $a = 2.5 \times 10^{-10}$ m (cross-sectional diameter of a methylene group); $b = 1.0 \times 10^{-9}$ m (approximate persistence length of PTHF, calculated based on data in: Brandrup, J. et al. In *Polymer Handbook*, 4th ed.; John Wiley & Sons, Inc.: Hoboken, NJ, 1999) and $S = 1$.